Research article

Tribological behavior and mechanical properties of friction stir processed HDPE/Fe-Fe$_3$O$_4$ composites

Saeed Karimi [a], **Seyed Mohammad Arab** [b,*], **Seyyed Reza Hosseini Zeidabadi** [c], **Sirus Javadpour** [c]

[a] *Technical Services Department, Pars Petrochemical Company, Asaluyeh, Iran*

[b] *Department of Mechanical Engineering, University of Mohaghegh Ardabili, P.O. Box 179, Ardabil, Iran*

[c] *Department of Materials Science and Engineering, School of Engineering, Shiraz University, Shiraz, Iran*

ABSTRACT

In the current work, high density polyethylene (HDPE) composites were fabricated via Friction Stir Processing (FSP). A two-phase Fe-Fe$_3$O$_4$ powder was used as the reinforcing agent. The extremely low cost powder was obtained from shot-blasting of as-forged low carbon steel components. X-ray diffraction (XRD) was used to phase analysis and evaluation of the purity of the as-received powder. The size distribution of the powder was determined by Laser Particle Size Analysis (LPSA). Also, Scanning Electron Microscopy (SEM) was employed to investigate the particles morphology. The processing used a cylindrical tool to impose the severe plastic deformation and material stirring in order to improve the mechanical properties and particles distribution. The tribological and mechanical properties of the fabricated samples were examined. According to the results, both the friction coefficient and specific wear rate of FSPed samples reduced remarkably. The hardness and tensile strength of the FSPed composites were higher than the FSPed HDPE samples; however, their elongations were lower.

© 2021 The Authors. Published by Synsint Research Group.

1. Introduction

The low permeability, low friction coefficient, high chemical resistance, and moderate mechanical properties have made high density polyethylene an applicable low-cost thermoplastic material. It is used in a variety of applications including water and food storage containers, chemical storage tanks, pipes, natural gas transportation, short-term load-bearing films, trash cans, and toys [1]. However, the main limitations of HDPE are its low scratch resistance, high coefficient of thermal expansion, and great care required for welding/processing [2]. Various metal-oxide reinforcing particles have been used to improve physical [3], thermal [4], mechanical [5], thermo-mechanical [6], and tribological [7] properties of HDPE. The shot blasting process is used to remove surface oxides, improve surface finish and enhance the

fatigue resistance of the metallic components [8]. Although the obtained Fe-Fe$_3$O$_4$ powder is very cheap, the recycling or reduction to iron is not cost-effective and also the free oxide dusts could lead to serious health problems [9]. Hence, there could be a potential to use the as-received powders for value-added applications such as composite making.

Friction Stir Welding (FSW) has been invented by The Welding Institute (TWI-UK) in 1991 [10]. Mishra et al. [11] developed Friction Stir Processing (FSP), which has been used to fabricate various metal surface composites. In the FSW and FSP, intensive strains and material's mixing take place by using a rotating tool which includes different geometries of shoulder patterns and pin [12]. These techniques have been also employed successfully to disperse micro and nano-sized reinforcing agents into the thermoplastic polymers, mainly

HDPE (nano-clay and micro-copper) [13, 14], polypropylene (nano-Al_2O_3) [15], and nylon 6 (multi wall carbon nanotube) [16]. However, the majority of FSP and FSW studies have been restricted to evaluate and optimize the effects of joining and processing parameters on the final properties of the thermoplastics including HDPE [17], polypropylene [18], nylon 6 [19], and acrylonitrile butadiene styrene [20].

In the current work, HDPE sheets have been reinforced with 2-phase micro-particles of iron-iron oxide (Fe-Fe_3O_4) provided from shot blasting of as-forged low carbon steel components via FSP. The tribological behavior and mechanical properties of the samples (as received HDPE, FSPed HDPE, and FSPed HDPE/Fe-Fe_3O_4) investigated by means of pin-on-disk, tensile and hardness tests.

2. Materials and method

2.1. Raw materials and equipment

The 5 mm thick HDPE sheets (99.9% pure fabricated by TEPHLON Co.) and Fe-Fe_3O_4 micro-powder were considered as the matrix and reinforcement, respectively. The powder was obtained from the surface shot blasting of as-forged low carbon steel components. The H13 tool steel cylindrical FSP tool including a pin (5 mm in diameter and 3 mm in height) and a concaved shoulder (20 mm in diameter) was made to fabricate surface composites. A universal milling machine (TABRIZ-FP4M) was used to fabricate the samples. The X-ray diffraction spectrometer (XRD: Phillips-PW1720), laser particle size analyzer
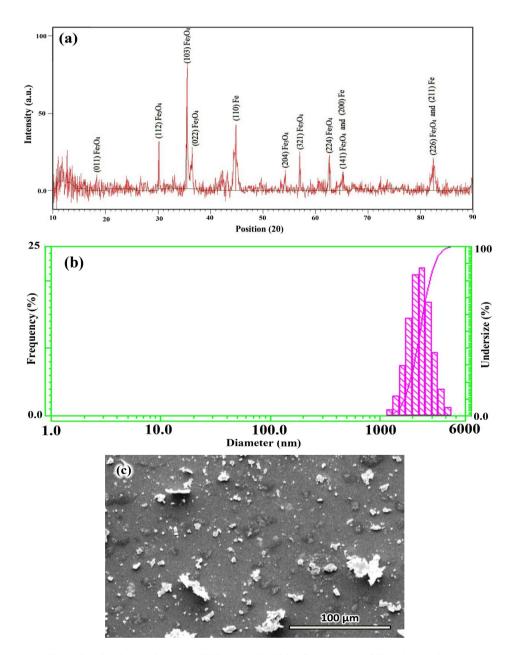

Fig. 1. Powder characterization: a) XRD pattern, b) LPSA diagram, and c) SEM micrograph.
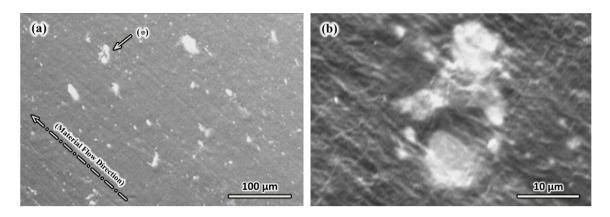
Fig. 2. Surface SEM micrographs of the sample "C": a) powder alignment, b) particle "*" in a higher magnification.

(LPSA: Horiba-LB550), scanning electron microscope (SEM: Cambridge-360), a conventional pin-on-disk test machine, hardness tester (Santam-Shore-D), and universal tensile test machine (Santam-STM150) were used to characterize the samples.

2.2. Powder characterization

The Fe-Fe$_3$O$_4$ powder was screened through a 400 vibrating mesh screen to obtain particle size lower than 37 μm. Then XRD, LPSA and SEM were employed to evaluate the purity, investigate the particle size distribution and study the powder morphology, respectively.
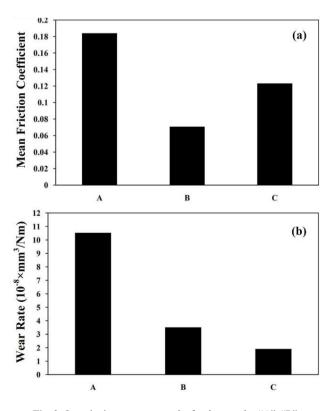

Fig. 3. Quantitative wear test results for the samples "A", "B", and "C": a) mean friction coefficient, b) wear rate.

2.3. Friction stir processing

First, 5 mm thick HDPE sheets were cut to 100×100 mm^2 pieces. The three parallel slots were machined on the polymer sheets (1 mm in width and 2 mm in depth) and then the reinforcement was filled into them, the slots were closed with a thin layer of molten HDPE to prevent splashing out of the powder during FSP. Several processing parameters were examined and the optimum one was chosen based on the smoothness of the sound samples. Finally, five similar surface composite and pure HDPE samples were processed with the rotational and traverse speeds of 630 RPM and 12 mm/min and a tilt angle of 2 °. Table 1 presents the studied samples and their assigned codes.

2.4. Wear test

The pin-on-disk wear examinations were carried out based on ASTM G99-04 at room temperature under 10 N normal load, 0.041 m/s of linear sliding speed, using a hard steel pin for 300 m of wear path. The samples surfaces were polished by the ultra-smooth grinder, cleaned by ethanol, and weighed before and after the test by means of a precise balance (0.0001 g). The instantaneous friction coefficient was measured and the specific wear rate was calculated by Eq. 1 as following [21]:

$$W_R = \frac{\Delta m}{\rho LF} \times 10^3 \tag{1}$$

where, W_R (mm^3/Nm), Δm (g), ρ (g/cm^3), L (m), and F (N) are specific wear rate, weight loss, density, wear distance, and applied force, respectively. The density of the raw materials and the fabricated composites were determined by the Archimedes method. The required data are presented in Table 1. Eventually, the worn surfaces were studied by SEM.

Table 1. Density and weight loss of the samples and their assigned codes.

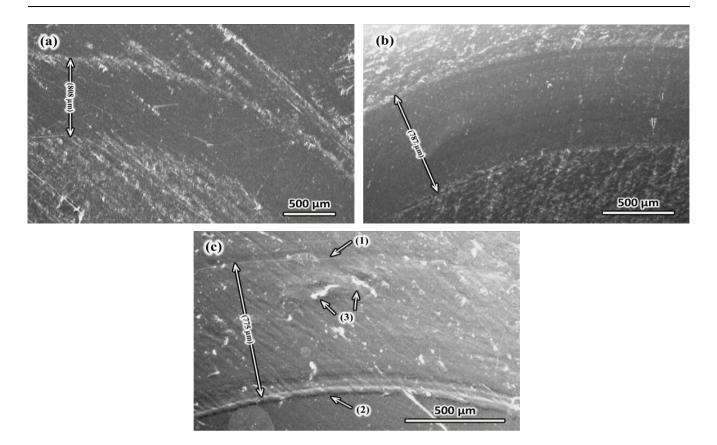| Δm (g)	ρ (g/cm^3)	Sample	Code
0.0003	0.95	Pristine HDPE	A
0.0001	0.95	FSPed HDPE	B
0.0001	3.50	FSPed HDPE/Fe-Fe$_3$O$_4$	C

Fig. 4. SEM micrographs of the wear path (samples "A", "B", and "C").

2.5. Hardness test

Shore-D hardness test was carried out based on ASTM D2240-05 at room temperature to obtain the surface hardness profile (Fig. 6).

2.6. Tensile test

To examine the tensile properties of the surface composites, the tensile specimens were machined just from the stir zones of the FSPed samples. The tests were conducted based on ASTM D638-03 (Type II).

3. Results and discussion

3.1. Powder characterization

Fig. 1a shows the XRD pattern of the as-received powder. Iron (Fe) and iron oxide (Fe_3O_4: magnetite) are present. The stronger peaks show the most of the oxide layers during forging process are composed of Fe_3O_4. The remained Fe comes from the inner layers of oxide scales or is caused by the removal of thin layers of Fe from the surface of parts during shot peening. The LPSA diagram (Fig. 1b) indicates a normal powder distribution with an average particle size of 2.5 μm. The SEM micrograph of the powder (Fig. 1c) supports the LPSA results and reveals its flaky morphology including some elongated, agglomerated and equiaxed particles.

3.2. Assessment of the fabricated composites

Fig. 2 represents the SEM micrographs of the FSPed composites. It is seen that the particles have a uniform distribution and are orientated along the material flow direction (Fig. 2a). The asterisk symbol of Fig. 2a represents an agglomerated particle, which is shown in higher magnification in Fig. 2b which shows an appropriate bonding to the matrix and there is no de-bonded interface or micro-cracks. This improves the mechanical and tribological properties of the composites.

3.3. Tribological analysis

3.3.1. Quantitative evaluation

The sample "B" indicates a 60% reduction of friction coefficient (Fig. 3a). The $Fe-Fe_3O_4$ particles are dispersed into the sample "C" through FSP and have decreased the coefficient of friction about 30% in comparison with sample "A.

The specific wear rates were calculated through Eq. 1 based on Table 1 data. The results are presented in Fig. 3b. The sample "C" shows the minimum wear rate (1.90×10^{-8} mm^3/Nm), more than 80% lower than that of sample "A" (10.53×10^{-8} mm^3/Nm). The wear rate of the sample "B" (3.51×10^{-8} mm^3/Nm) is also decreased about 65% compared to the sample "A". The hard particles and FSP itself lead to a synergistic effect on decreasing the wear rate.
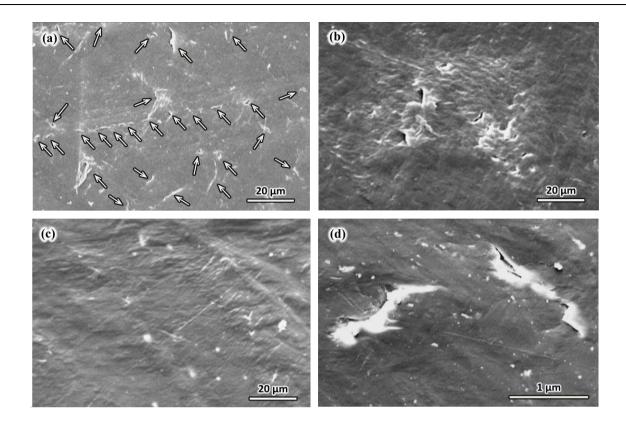
Fig. 5. SEM micrographs of the wear beads for: a) sample "A", b) sample "B", c) sample "C", and d) sample "C" in a higher magnification (marked as region 3 in Fig. 4c).

3.3.2. Qualitative evaluation

The worn surface of the A, B, and C samples are illustrated in Fig. 4. The micrographs reveal that the widths of the worn path are decreased from sample "A" to "C". Some convexities (region 1) and concavities (region 2) can be observed on the path edge in Fig. 4c, which are evidence for micro-plowing mechanism of abrasion wear [22]. The lower wear rate of the sample "C" is explained by activation of the mentioned mechanism so that the worn material has been pushed and plowed toward the path edge instead of chipping and throwing away. Micro-cutting is another activated wear mechanism, which could be traced by the scratches in the vicinity of worn edges [23]. As Fig. 4 shows, the scratches actually have been created by rubbing the hard Fe-Fe_3O_4 particles on the HDPE matrix; therefore, these phenomena could not be seen in the "A" and "B" samples.

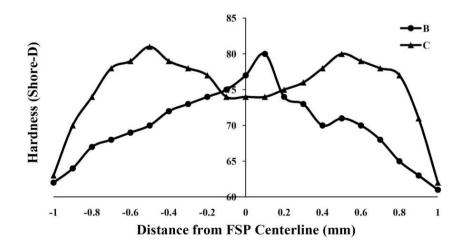Fig. 5 shows the SEM micrographs of the worn surfaces. The three first

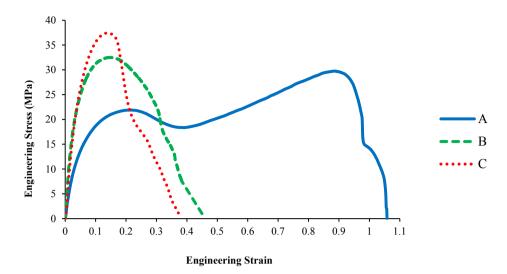**Fig. 6.** Hardness variation profile for the samples "B" and "C".

Fig. 7. Engineering stress-strain curves for the samples "A", "B," and "C".

ones are captured in the same magnification for better comparison. The network of transverse and longitudinal micro-cracks could be observed in the "A" sample (Fig. 5a). As Fig. 5b reveals, there are some micro-cracks on the Sample "B" worn surface; however, their population is less than sample "A" and they are more localized with wider crack openings. This may be resulted from strength improvement (section 3.4.2), which could impede the crack nucleation and propagation. The plastically deformed surface could introduce the adhesion as governing wear mechanism.

There is no evidence of micro-cracks on the worn surface of the sample "C" (Fig. 5c); which has the highest strength and hence the highest resistance against crack nucleation and surface fatigue [24]. Besides, Fig. 5d shows some micro-cracks at the higher magnification (marked as region 3 in Fig. 4c), especially in the particle-matrix interface and also among the agglomerates. It could verify the dominance of the adhesion mechanism; thus, a complex mechanism of abrasion/adhesion has been activated.

3.4. Mechanical properties

3.4.1. Hardness evaluation

Fig. 6 represents the Shore-D hardness profiles for different samples. The hardness of the FSPed samples is higher than that of the pristine HDPE (equal to 67 Shore-D). The hardness variation of the sample "B" is completely different from the sample "C". Maximum hardness of the sample "B" is observed in the centerline. It could be attributed to asymmetric and non-uniform material flow in the stir zone. The hardness profile of the sample "C" is M-shape: one minimum exactly under the pin and two maximums near the pin's periphery. This could be resulted from powder accumulation around the pin, which may increase the matrix hardness.

The hardness of the regions far from the FSP line of the samples "B" and "C" is lower than that of the sample "A", which could be due to the temperature elevation, creation of a mushy state without an applied external load, non-uniform distribution of materials around the pin, and formation of defects such as voids and channels [14]. The mean hardness value of the sample "C" (75 Shore-D) is about 11% and 9% higher than the hardness of sample "A" (67 Shore-D) and "B"

(69 Shore-D), respectively. The hardness improvement of the sample "C" could increase its resistance against indentation of the wearing pin. Therefore, the width of worn path is reduced and its wear rate is decreased according to the Archard classic theory, which implies wear rate reduction by increase of the material hardness [25].

3.4.2. Tensile behavior

Tensile specimens were extracted from the center of FSPed line to obtain the mechanical properties of stir zone. The engineering stress-strain curves of the "A", "B", and "C" samples are shown in Fig. 7. The FSP could twist, twin and somehow tie the HDPE polymer chains. The mechanical locks of the thermoplastic chains improve the tensile strength on one hand and reduce the capability of chain aligning and elongating on the other hand. The tensile strength of the sample "B" has been increased 13% at the expense of elongation reduction for about 57%. These values are 25% and 60% for the sample "C", respectively. The enhancement of tensile strength has two main reasons, severe plastic deformation by FSP and formation of an appropriate Fe_3O_4/HDPE interface.

4. Conclusions

- According to the results, FSP of HDPE could be introduced as a good approach for improving the hardness and tensile strength as well as the wear resistance.

- The FSP of pristine HDPE and making composites could reduce the friction coefficient and wear rate and also could increase the hardness and tensile strength. An appropriate dispersion of the particles and formation of an acceptable phase interface could be introduced as the exclusive properties of the fabricated composites.

- The microscopic observations of the worn surface revealed the activation of the adhesion mechanism for both pristine and FSPed HDPE; while, a complex abrasion/adhesion mechanism was activated in the fabricated composite.

- Eventually, the Magnetite powder could be introduced as a cost-effective and efficient reinforcing agent to increase the mechanical and tribological properties of HDPE sheets by FSP.

References

[1] A. Peacock, Handbook of polyethylene: structures: properties, and applications, CRC Press, New York. (2000) 2–3. https://doi.org/10.1201/9781482295467.

[2] J. Scheirs, A guide to polymeric geomembranes: a practical approach, Wiley, London. (2009) 55–56.

[3] M.T. Sebastian, H. Jantunen, Polymer–ceramic composites of 0–3 connectivity for circuits in electronics: a review, Int. J. Appl. Ceram. Technol. 7 (2010) 415–434. https://doi.org/10.1111/j.1744-7402.2009.02482.x.

[4] R.H. Elleithy, I. Ali, M.A. Ali, S.M. Al-Zahrani, High density polyethylene/micro calcium carbonate composites: A study of the morphological, thermal, and viscoelastic properties, J. Appl. Polym. Sci. 117 (2010) 2413–2421. https://doi.org/10.1002/app.32142.

[5] S. Ersoy, M. Taşdemir, Zinc oxide (ZnO), magnesium hydroxide [$Mg(OH)_2$] and calcium carbonate ($CaCO_3$) filled HDPE polymer composites, Mechanical, thermal and morphological properties, Fen Bilim. Derg. 24 (2012) 93–104.

[6] H. Fouad, R. Elleithy, O.Y. Alothman, Thermo-mechanical, wear and fracture behavior of high-density polyethylene/hydroxyapatite nano composite for biomedical applications: effect of accelerated ageing, J. Mater. Sci. Technol. 29 (2013) 573–581. https://doi.org/10.1016/j.jmst.2013.03.020.

[7] S. Bodhak, S. Nath, B. Basu, Friction and Wear Properties of Novel HDPE–HAp–Al2O3 Biocomposites against Alumina Counterface, J. Biomater. Appl. 23 (2009) 407–433. https://doi.org/10.1177/0885328208090012.

[8] D.M. Kennedy, J. Vahey, D. Hanney, Micro shot blasting of machine tools for improving surface finish and reducing cutting forces in manufacturing, Mater. Des. 26 (2005) 203–208. https://doi.org/10.1016/j.matdes.2004.02.013.

[9] N. Lewinski, H. Graczyk, M. Riediker, Human inhalation exposure to iron oxide particles, BioNanoMaterials. 14 (2013) 5–23. https://doi.org/10.1515/bnm-2013-0007.

[10] W.M. Thomas, J.C. Needham, M.G. Murch, P. Templesmith, C.J. Dawes, Friction stir welding; International Patent Application No. PCT/GB92/02203 and GB Patent Application No. 9125978.8 and US Patent Application No. 5,460,317 (1991).

[11] R.S. Mishra, Z.Y. Ma, I. Charit, Friction stir processing: a novel technique for fabrication of surface composite, Mater. Sci. Eng. A. 341 (2003) 307–310. https://doi.org/10.1016/S0921-5093(02)00199-5.

[12] S.M. Arab, S. Karimi, S.A.J. Jahromi, S. Javadpour, S.M. Zebarjad, Fabrication of novel fiber reinforced aluminum composites by friction stir processing, Mater. Sci. Eng. 632 (2015) 50–57. https://doi.org/10.1016/j.msea.2015.02.032.

[13] M. Barmouz, J. Seyfi, M.K.B. Givi, I. Hejazi, S.M. Davachi, A novel approach for producing polymer nanocomposites by in-situ dispersion of clay particles via friction stir processing, Mater. Sci. Eng. 528 (2011) 3003–3006. https://doi.org/10.1016/j.msea.2010.12.083.

[14] E. Azarsa, A. Mostafapour, On the feasibility of producing polymer–metal composites via novel variant of friction stir processing, J. Manuf. Process. 15 (2013) 682–688. https://doi.org/10.1016/j.jmapro.2013.08.007.

[15] S. Alyali, A. Mostafapour, E. Azarsa, Fabrication of PP/Al2O3 Surface Nanocomposite via Novel Friction Stir Processing Approach, Int. J. Adv. Eng. Tech. 3 (2012) 598–605.

[16] R. Farshbaf Zinati, Z. Zhou, Finite element simulation of material flow in friction stir process of nylon 6 and nylon 6/MWCNTs composite, Cogent. Eng. 2 (2015) 1–24. https://doi.org/10.1080/23311916.2015.1048098.

[17] M.K. Bilici, A.I. Yukler, Effects of welding parameters on friction stir spot welding of high density polyethylene sheets, Mater. Des. 33 (2012) 545–550. https://doi.org/10.1016/j.matdes.2011.04.062.

[18] Z. Kiss, T. Czigány, Applicability of friction stir welding in polymeric materials, Period. Polytech. Mech. Eng. 51 (2007) 15–18. https://doi.org/10.3311/pp.me.2007-1.02.

[19] I.M. Husain, R.K. Salim, T. Azdast, S. Hasanifard, S.M. Shishavan, E.E. Lee, Mechanical properties of friction-stir-welded polyamide sheets, Int. J. Mech. Mater. Eng. 10 (2015) 1–8. https://doi.org/10.1186/s40712-015-0047-6.

[20] A. Bagheri, T. Azdast, A. Doniavi, An experimental study on mechanical properties of friction stir welded ABS sheets, Mater. Des. 43 (2013) 402–409. https://doi.org/10.1016/j.matdes.2012.06.059.

[21] C. Lhymn, Y. Lhymn, Friction and wear of rubber/epoxy composites, J. Mater. Sci. 24 (1989) 1252–1256. https://doi.org/10.1007/PL00020203.

[22] Z. Chen, T. Li, X. Liu, R. Lü, Friction and wear mechanisms of polyamide 66/high density polyethylene blends, J. Polym. Sci. B: Polym. Phys. 43 (2005) 2514–2523. https://doi.org/10.1002/polb.20548.

[23] N. Chand, A. Naik, Development and high stress abrasive wear behavior of milled carbon fiber-reinforced epoxy gradient composites, Polym. Compos. 29 (2008) 736–744. https://doi.org/10.1002/pc.20450.

[24] P.V. Vasconcelos, F.J. Lino, A.M. Baptista, R.J.L. Neto, Tribological behaviour of epoxy based composites for rapid tooling, Wear. 260 (2006) 30–39. https://doi.org/10.1016/j.wear.2004.12.030.

[25] M.B. Peterson, W.O. Winer, Wear control handbook, American Society of Mechanical Engineers (ASME). (1980) 62–65.